Metamaterial Structures for Compact Millimeter Wave Antenna Applications

Cuong Tran Manh[1], **Habiba Hafdallah Ouslimani**[1], **Geraldine Guida**[1]
Alain Priou[1], **Herve Teillet**[2], **and J. Y. Daden**[2]

[1]Applied Electromagnetic Group (GEA), Université Paris X, Nanterre
50 rue de Sevres, Ville d'Avray 92410, France
[2]THALES Communications, 160 Boulevard de Valmy, Colombes 92704, France

Abstract— This paper proposes the study of some high impedance surface (HIS) structures for compact antenna applications in the millimeter-wave domain. The millimeter wave domain is now very important for high speed wireless and high bit rate optical (> 40 Gbits/s) communications systems. The HIS structures provide many advantages for antennas as they enhance their performances; HIS structures have capability to block the surface wave, to reduce the coupling effect, to present high real impedance at the resonance frequency ($R_e(Z) \gg 377\Omega$) and to reduce the global thickness of the low profile antenna. Several high impedance surfaces structures are analyzed and their properties compared. We perform this analysis on structures which composed of rectangular lattices patches periodic arrangements, Jerusalem lattices shape and 2LC shape (two LC split loops). For each structure, we are interested in the frequency behavior of the reflection phase to determine the resonance frequency and the band-gap as well as in the losses (joule effect) in the structure. All the dimensions and shapes of the unit cell geometry are optimized in order to use the dielectric substrate available in our laboratory. The high impedance surface is modeled using HFSS (Ansoft) code based on finite element methods. We chose the structure presenting the best performances to design the metamaterial antenna with coaxial feed and finite surface witch is modeled with 7×7 and 9×9 double rang unit cells. In comparison with conventional antenna type, placed above a metal ground plan, the antenna placed above the HIS has smoother radiation profile, less power wasted in the backward direction, better return loss (at least -10 to -15 dB better) and higher gain and directivity (at least $+1$ dB). The layout of the HIS structures circuits (many varieties) are now edited and the manufacturing process in progress. The results of the HFSS simulations will be compared with the experimental free space and coaxial measurements in the millimeter-wave domain.

1. INTRODUCTION

We have known that a patch antenna consist of a metal patch suspended over a ground plane and separate with the ground plane by a dielectric substrate, so is acts as a cavity. We use herein the rectangular shape for radiator patch, and we choose the coaxial feeding method, the feeding point has chosen at the patch's corner in the purpose of impedance matching. Antennas of this type are low-profile but highly resonant.

In the circuit, the ground plane is always finite, and its edges contribute to the radiation pattern. In addition to space waves, the antenna generates surface waves in the ground plane, which then radiate from edges and corners. The combined radiation from the patch and the ground plane edges interfere to form a series of multipart lobes and nulls at various angles. The edges radiate backwards as well as forwards, causing a significant amount of wasted power in the backward hemisphere and ripples in the antenna pattern. This problem is exacerbated, if the substrate is thick, or has a high dielectric constant.

Many authors propose the suppression of the surface waves, by embedding the patch antenna in a highimpedance ground plane as [1–5]. In the following example (Fig. 1), D. Sievenpiper shows a comparison between the radiation pattern of a microstrip patch and HIS ground plane patch antenna.

The measurements (Fig. 1) are at a frequency in which the two antennas have the same return loss. In both the H and E-plane, the patch on the ordinary metal ground plane shows significant radiation in the backward direction, and ripples in the forward direction. The pattern is not rotationally symmetric, and is much thinner in the H-plane than in the E-plane. Conversely, the patch placed over the high-impedance ground plane produces a smooth, symmetric pattern with little backward radiation.

In this paper, after presenting some potential planar microstrip high impedance surfaces and their frequency response, we chose the structure presenting the best performances, to design the

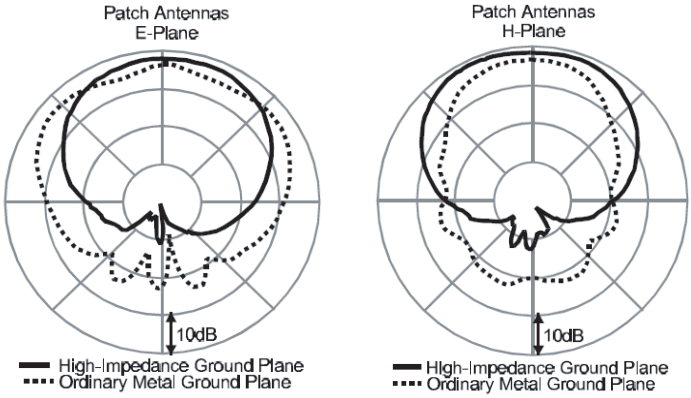

Figure 1: E and H-plane radiation patterns of two patch antennas [1].

metamaterial antenna with coaxial feeding method and finite ground plane surface. The later is modeled with 7×7 double rang unit cells. In comparison with conventional antenna type placed above a metal ground plan, the antenna placed above the HIS has smoother radiation profile, less power wasted in the backward direction, better return loss (at least -4 dB to -8 dB better) and higher gain and directivity (at least $+4$ dB)

2. HIS DEFINITION

High Impedance Surface (HIS) structures, also designed as Artificial Magnetic Conductor (AMC) or Perfect Magnetic Conductor (PMC) [3, 6] may be very useful for antenna applications and in a very large variety of microwave other devices [4, 5]. Electromagnetic band gap structures (EBG) have been widely studied for their behaviour as High Impedance Surface (HIS), since they show a stop band frequencies behaviour. The AMC condition is characterized by a resonance frequency where the phase of the reflection coefficient is zero and its magnitude equal to one. In contrast, an HIS may deviate a little from this condition, sometimes yielding more flexibility in antenna design. In this case, we defined a band gap frequency as a frequency range in which the reflection phase cross from $+90°$ to $-90°$ [9].

Like the proposition of Sievenpiper and co-others [1, 4], planar periodic array of metallic patches with connection via to the ground plane exhibit a high impedance with an exactly zero degree reflection phase at the resonance frequency. Array of patches without via connection to the ground plane exhibit also this property. We have known that, there is a problem with most of proposed HIS structures because they present a shift of the resonant frequency versus the incidence angle [15].

3. SIMULATION MODEL OF HIS STRUCTURES

3.1. HFSS Modelling

The performances of the HIS structures are studied using numerical simulation from a finite element method HFSS codes (FEM-HFSS ANSOFT Version 10.1). We use three structures: the square patches structure, the Jerusalem structure and the two LC boucles "2LC" structure. The Figure 2 (below) gives the studied planar structures called also Uni-planar Compact Photonic Bandgap

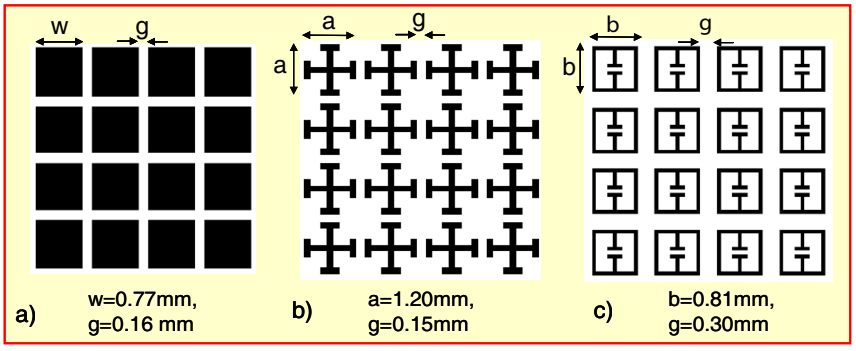

Figure 2: Square patches (a), Jerusalem (b) and the "2LC" (c) structures.

(UCPBG) [10, 11].

Patch antennas are studied with all the three type of HIS structure listed above. The simulation set-up is presented in Figure 3. A plan wave model is established to evaluate the reflection phase of the EBG surface. The plan wave is launched to normally illuminate the EBG structure like the method in [7] and [12]. To model an infinite periodic structure, we used a single unit of EBG structure with periodic boundary condition on the four sides of the sample in simulation.

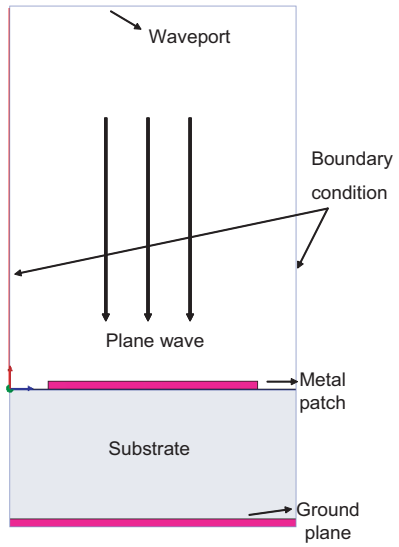

Figure 3: Setup simulation for one cell "UCPBG".

3.2. Numerical Results

The geometries (all dimensions) of the three types of structures are optimized in the millimeter wave domain, corresponding to the 40–45 GHz frequency range. The used substrate has the following characteristics: thickness $h = 0.51\,\text{mm}$, permittivity $\varepsilon = 3.38$ (RO4003 substrate) and $\tan(\delta) = 0$. The metallic cell patches and ground plan are chosen to be perfect electric conductor (no loss in the material).

The optimized dimensions for the unit cell and the array period for the three structures are respectively; $W \times W = 0.7742 \times 0.7742\,\text{mm}^2$, array period $P = 0.931\,\text{mm}$ for the rectangular patch, array period $P = 1.11\,\text{mm}$ for the "2LC" and array period $P = 1.30\,\text{mm}$ for the Jerusalem structure.

The obtained results on the optimized structures are shown in Figure 4. For each type, we can see the diagram of return loss, the reflection phase and the real and imaginary part of the surface impedance.

Broader band gap results in a better control of the antenna backward radiation, thus it is essential to choose the structure which shows the largest band gap. We know also, that the band gap will be seriously reduced for incoming plane wave with a certain incidence angle. In our simulation, the chosen structure showed the best real part of surface impedance approximately $6 \cdot 10^4\,\Omega$. After analysis, we show that the rectangular HIS structure presented the best performances for antenna.

Table 1: For the different cells: the resonance frequency, the bandgap width and the dimension period.

Type of structure	Period(mm)	Frequency(GHz)	Bandwidth(%)
Rectangular	0.93	41.2	41.46
Jerusalem	1.30	40.6	27.16
2LC	2.04	41.5	22.89

At the resonance frequency, the reflection coefficient has zero-phase and the surface impedance is real and maximum (infinite in theory). For all three structures, the minimum return loss occurs

approximately at the resonance frequency. The relative bandwidth of the three structures is defined as:

$$B_{\text{bandwidth}} = \left(f_{[+90^\circ]} - f_{[-90^\circ]}\right) / f_{[0^\circ]}$$

And the results are reported in Table 1.

One can observe that, the rectangular patch HIS presents the best results in term of band gap width, stability and satisfied features for antenna application. It was naturally chosen to simulate the antenna performances. In order to verify the constancy of the resonance frequency, particularly when the unit cell is integrated to the array and when it interact with the other cells, we have simulate new patches structures with lager number of elements (4×4 to 6×6). The results showed that the bandgap region does not shift since the period of structure remains exactly the same (imposed by the unit cell).

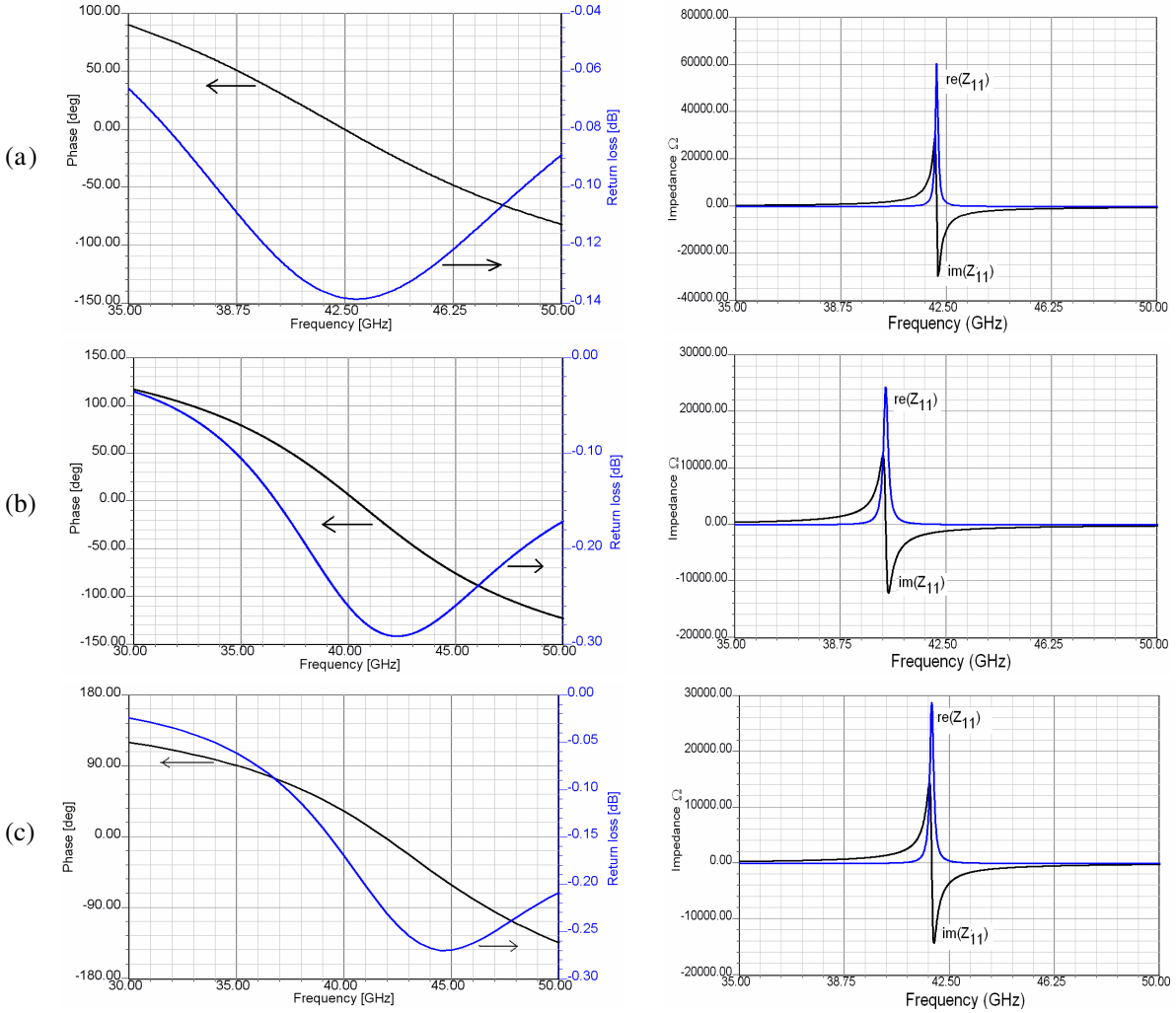

Figure 4: Numerical simulation results: (a) Rectangular, (b) Jerusalem and (c) "2LC" patches. Left: Return loss magnitude (dB) and phase (degrees). Right: Impedance surface $\mathrm{Z_{in}}(f)$.

4. ANTENNA PATCH SIMULATION WITH AND WITHOUT HIS STRUCTURE

Figure 5 shows the antenna topology that we choose to study in this paper. Following the analysis and results obtained in Section 3, we use the high impedance surface, rectangular type to realize our antenna. Using this "composite" ground plan structure, we expect better performances (enhance of the antenna gain, directivity and return loss). All the results presented here compare the performances of the two types of ground plan structures; conventional antenna and HIS antenna (metamaterial antenna).

The radiator element is exactly the same in the two antennas (rectangular patch antenna of 1.75×1.60 mm and 0.03 mm copper thickness). The radiator element is fed using coaxial line and

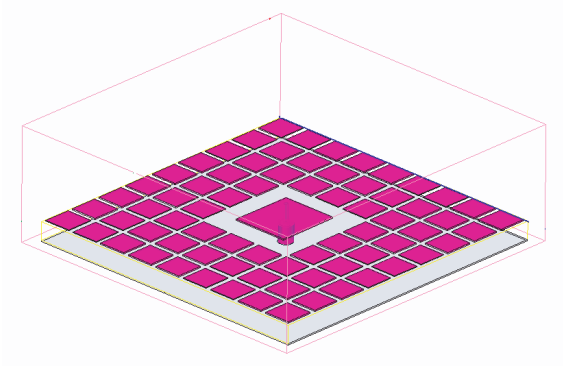

Figure 5: A patch antenna embedded in a high-impedance ground plane.

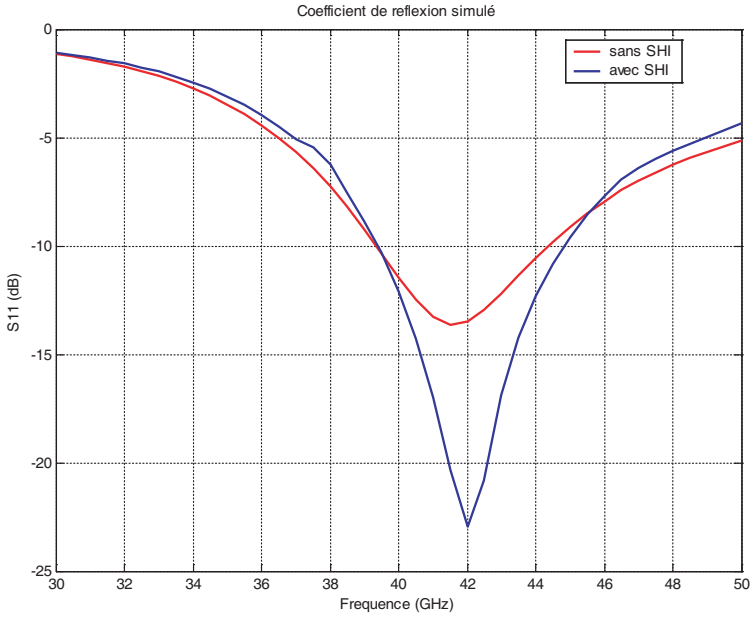

Figure 6: Comparison of the return loss (MS_{11}) between HIS ground plane and conventional patch antennas.

positioned in order to obtain the best impedance matching (0.2 mm at the corner of radiator).

We have show here in the Figures 7 and 8 the simulation results of two antennas at 42 GHz, the point in which both of them have the same value of return loss (see the Figure 6), the comparison in

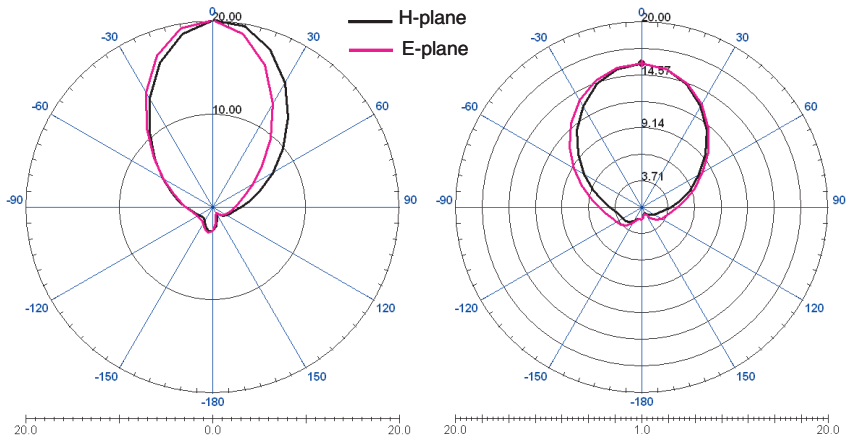

Figure 7: Radiation pattern comparison of two kinds of antenna at 42 GHz.

Figure 8 has shown clearly the advantage of using HIS structure for patch antenna; We receive the augmentation 4.5 dB of gain and/or directivity for patch with HIS in our simulation (see Figure 8) compared with the conventional patch, thus leading to an increase in bandwidth and efficiency of antenna [14]. From the Figure 7, we see that the radiation pattern of the metamaterial antenna is more directive (+20 dB) than the conventional antenna (+15 dB).

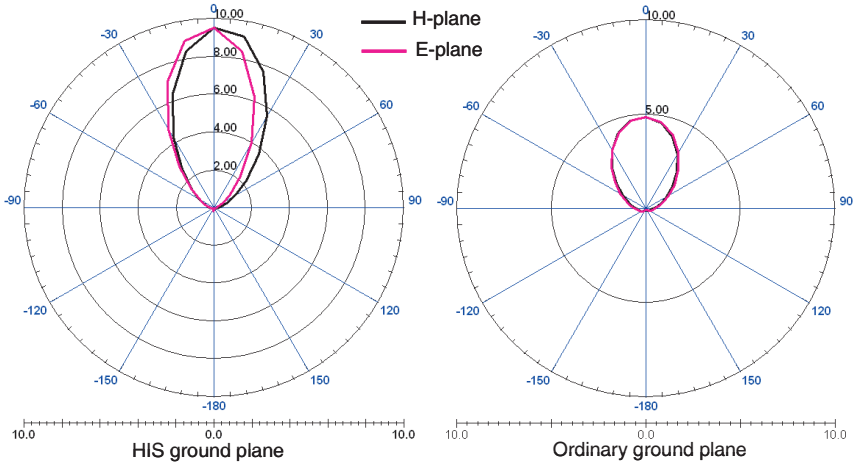

Figure 8: Gain/Directivity comparison of two kinds of antenna at 42 GHz.

5. CONCLUSIONS

We have used finite element method (FEM) to numerically determined characteristics of high impedance surface structures. Numerical results for return loss, reflection phase and input impedance are shown. The structure which shows the best performance is chosen to design a metamterial patch antenna. The results confirm and show the good characteristics of antenna with HIS ground plane. We have seen that, around of the resonant frequency, the return loss of the designed antenna decrease significantly and its gain and directivity are notably improved or enhanced.

The layout of many varieties of HIS structures circuits are now edited and the manufacturing process in progress. The comparison and discussion between the numerical results obtained by the simulation and experimental results will be presented in our future work.

REFERENCES

1. Daniel Sievenpiper Thesis, University California, Los Angeles, 1999.
2. Sievenpiper, D., L. Zhang, R. F. J. Broas, N. G. Alexopoulos, and E. Yablonovitch, "High impedance electromagnetic surfaces with a forbidden frequency band," *IEEE Trans., Micro., Theory Tech.*, Vol. 47, 2059–2074, 1999.
3. Yang, F. and Y. Rahmat-Samii, "Reflection phase characterizations of the EBG ground plane for low profile wire antenna applications," *IEEE Transacations on Antennas and Propagation*, Vol. 51, No. 10, 2003.
4. Gonzalo, R., P. de Maagt, and M. Sorolla, "Enhanced patch antenna performance by suppressing surface waves using photonic-bandgap substrates," *IEEE Transactions on Microwave Theory and Techniques*, Vol. 47, No. 11, 1999.
5. Cheype, C., C. Serier, M. Thèvenot, T. Monédière, A. Reineixn, and B. Jecko, "An electromagnetic bandgap resonator antenna," *IEEE Transactions on Antennas and Propagation*, Vol. 50, No. 9, 2002.
6. Kim, Y., F. Yang, and A. Z. Elsherbeni, "Compact artificial magnetic conductor designs using planar square spiral geometries," *Progress in Electromagnetics Research*, PIER 77, 43–54, 2007.
7. Schurig, D., J. J. Mock, and D. R. Smith, "Electric-field-coupled resonators for negative permittivity metamaterials," *Appl Physics Letter*, Vol. 88, 041109, 2006.
8. Abdelwaheb Ourir Thesis, University Paris X, 2006.
9. Engheta, N. and R. W. Ziolkowski, *Electromagnetic Metamaterials: Physics and Engineering Explorations*, Wiley-IEEE Press, August 2006.

10. Yang, L., M. Fan, and Z. Feng, "A spiral electromagnetic bandgap structure and its application in microstrip antenna arrays," *Microwave Conference Proceedings*, 2005.
11. J. M. Bell, M. F. Iskander, and J. J. Lee, "Ultrawideband hybrid EBG/Ferrite grounf plane for low-profile array antennas," *IEEE Transactions on Antennas and Propagation*, Vol. 55, No. 1, 2007.
12. Zheng, Q. R., B. Q. Lin, Y. Q. Fu, and N. C. Yuan, "Characteristics and applications of a novel compact spiral electromagnetic bandgap structure," *J. of Electromagn. Waves and Appl.*, Vol. 21, No. 2, 199–213, 2007.
13. Liu, C. H., Y. G. Lu, X. G. Luo, and C. L. Du, "The numerical simulation of AMC characteristics for UCPBG on grounded dielectric substrate," *J. of Electromagn. Waves and Appl.*, Vol. 21, No. 6, 755–768, 2007.
14. Alù, A., F. Bilotti, N. Engheta, and L. Vegni, "Subwavalength, compact, resonant patch antennas loaded with metamaterials," *IEEE Transactions on Antennas and Propagation*, Vol. 55, No. 1, 2007.
15. Hosseini, M., A. Pirhadi, and M. Hakkak, "A novel AMC with little sensitivity to angle of incidence using an optimized jerusalem cross FSS," PIER 64, 43–51, 2006.